www.amlett.com, www.amlett.org, DOI: 10.5185/amlett.2012.ib.103
"Nanostructuring by electrons, photons and ions" Special Issue Published online by the VBRI press in 2013

Low energy bombardment induced formation of Ge nanoparticles

Indra Sulania[1,2*], Dinesh Agarwal[1], Manish Kumar[1], Mushahid Husain[2], D.K. Avasthi[1]

[1]*Inter University Accelerator Centre, New Delhi 110067, India*
[2]*Jamia Millia Islamia, New Delhi 110025, India*

[*]Corresponding author. Tel. (+91) 11 26893955; Fax: (+91) 11 26893666; E-mail: indra.sulaniya@gmail.com, indra@iuac.res.in

Received: 16 March 2012, Revised: 22 July 2012 and Accepted: 26 July 2012

ABSTRACT

We present the formation of Ge nanostructures by bombardment of 1.5 keV Ar atoms on Ge (100). The bombardment was carried out at normal incidence with variation in the fluences from $5x10^{15}$ to $3x10^{17}$ atoms/cm^2. Near surface chemical study on the pristine and irradiated Ge samples has been carried out using X-ray Photoelectron Spectroscopy. In the near surface region of pristine sample, prominence of Ge^{4+} was observed by 3d core level present at a binding energy of 33.5 eV. After the irradiation, the evolution of two new core level peaks at binding energies of 29.8 and 30.4 eV confirms the reduction of Ge^{4+} to elemental Ge. Atomic Force Micrographs show an increase in surface roughness from 0.4 nm to 10 nm for pristine to sample irradiated at highest fluence. Using the scaling laws and calculating the roughness and growth exponents deduced from Power Spectral Density analysis, it has been found that ion induced coarsening leads to the surface roughening. Further, using the simulation code, it is found that with increasing fluence of bombardment, the deformation of surface starts initially which later on results in simultaneous formation of dots and pits. Copyright © 2013 VBRI press.

Keywords: Germanium; Ion Bombardment; Atomic Force Microscopy; X-ray Photoelectron Spectroscopy.

Indra Sulania is working as Scientist at IUAC, New Delhi. She is mainly working on Scanning Probe Microscope facility. Her area of research interest is the investigations of nanostructures formation on various materials and thin films due to low energy ion beams. These nanostructures include the nanoripples, nanodots, nanoholes etc.

D. K. Avasthi is working as Scientist at IUAC, New Delhi. He is the present group leader for materials Science Group and radiation biology group at IUAC, New Delhi. He has keen interest in Insitu/ Online measurements during ion irradiation like (i) Electronic sputtering by on-line ERDA (ii) Phase transformation and growth/reduction of nanoparticle size by in-situ XRD, (iii) on-line Measurement of gas release during ion irradiation (iv) In-situ raman spectrometer (being setup) Established role of thermal spike in SHI induced mixing in metal/Si and metal/metal systems. Synthesis and engineering of nanostructures by ion beams, ion beam interaction with nanodimensional systems, Synthesis of metal nanoparticles embedded in different matrices by atom beam co-sputtering and understanding of the same by simulation, Creation of functional surfaces by ion beams.

Manish Kumar received the Ph.D. degree in year 2010 from Department of Physics at Indian Institute of Technology. His Ph.D. thesis work was on '*Ag:ZrO_2 Nanocomposite Thin Films Synthesized by Sol-Gel Technique'* carried out in 'Thin Film Laboratory' under supervision of Professor G.B. Reddy. Since 2009, he has been working as Post-doctoral Fellow in Materials Science Group of Inter University Accelerator centre, New Delhi. His research interest includes Nanostructured materials and thin films for functional applications, Plasmonics, Surface-Interface studies and Ion-beam induced materials modification.

Introduction

Low-energy ions are used extensively for cleaning the semiconductor surfaces during device processing. During the process of etching, there is formation of various features on the surfaces with reduced size and better ordering. In 1956, Navez *et al.* observed for the first time that a new morphology on the surface of glass arises due to ion bombardment depending mainly on the incidence angle [**1**]. Later on, advanced processing techniques such as reactive ion-beam etching, ion-assisted deposition, direct ion deposition, and surface modification for tribological or corrosion-resistant applications, are actively being investigated and applied [**2, 3**]. These processes can benefit from a thorough understanding of physics of ion-surface interactions, defect production yields and defect annealing kinetics in order to apply it for controlled fabrication of surface nanostructures. During the process of low energy ion bombardment, the near surface region of the target material gets amorphized due to creation of point defects thus leads to the formation of nanostructures on the surface of a material through the process of self assembly [**2-6**]. The main mechanisms governing such changes on the surface is the competition/interplay between the roughening induced by ion bombardment and smoothening due to surface diffusion. Until now researchers have observed two different types of self-organized patterns during ion beam erosion: ripple and dot pattern [**7-12**]. Due to self-organization processes and for appropriate sputtering conditions, these patterns can show a very high degree of lateral ordering [**3, 13**].

Germanium (Ge) is considered to be a substitute to Si for next generation complementary metal oxide semiconductor devices because of their high intrinsic carrier mobility, and thus has attracted much interest recently [**14, 15**]. Ziberi et al. studied the nanostructure formation on Ge with 2 keV Ar ions. They observed a well-ordered dot formation at normal incidence which evolves into ripple formation as the angle of incidence was increased [**13**]. Floro et al. [**16**] studied the surface defect production on Ge (100) due to 70-500 eV Ar and Xe ions and found that Xe induces more defects on the surface upon bombardment than the Ar ions due to much higher mass. Also, at elevated substrate temperatures the observed surface defect yield is reduced for Ar and Xe bombardment, presumably by defect annealing. The kinetics of surface roughening of Ge (001) due to 200 eV Xe^+ ions bombardment has been studied by Chason et al. during the molecular beam epitaxy to see the surface diffusivity of Ge on Ge (100). It was found that the initially smooth surfaces reach a steady state roughness which depends on the temperature and incident ion adatom flux. In another work Chason et al. bombarded Ge (100) with 200 eV Xe^+ ions as a function of substrate temperature. They measured the activation energies of 0.8 eV for surface migration during the bombardment in the case of Ge [**14, 17, 18**]. It is argued that the annealing arises from direct surface recombination of point defects. Defects that reach the surface enhances the surface diffusion if sufficient thermal energy is available and either recombine with each other (adatom plus surface vacancy), or annihilate at ledge sites. Zhou et al. have studied the ripple formation on Ge using the focused ion beam at normal incidence with 30 keV Ga ions. They have found that the ripple orientation changes with ion fluence [**19**]. Miyawaki et al. have studied the bombardment of 600 eV Ar ions on Ge with simultaneous supply of Ni. They observed various structure formation like nanocone, nanoneedle etc on Ge. It was concluded that Ni acts as a seed for these structures to form [**20**]. All the above studies have been carried out at a very low energy regime of the ions or electrons (0.07 to 0.5 keV). In our study we have used 1.5 keV Ar atoms to study the nanostructure formation on the Ge (100) surface.

The reported works on low energy ion bombardment on Ge mainly highlights the role of defect formation and did not consider the formation of surface nanostructures due to the ion impact. In the present work, we investigated the evolution of surface nanostructures on Ge by low energy atom bombardment instead of ion bombardment. Further on the basis of Scaling laws and simulation, experimental results are explained.

Experimental

In the present experiment, 1.5 keV Argon (Ar) atoms have been used to bombard the samples of Ge (100) at normal incidence. The base pressure of the chamber was around $5x10^{-6}$ mbar and $3x10^{-3}$ mbar during bombardment. Bombardment was carried out at room temperature ~ 23°C. An atom fluence ranging from $5x10^{15}$ to $3x10^{17}$atoms/cm^2 was used during the experiment and the beam flux was ~ 15μA/cm^2. **Fig. 1** shows the schematic of the set up of the sputtering unit designed indigenously at IUAC, New Delhi [**21**]. It has a Argon source which delivers a current density of 30 μA/cm^2. The samples were mounted at the top part of the chamber as shown in the **Fig. 1**.

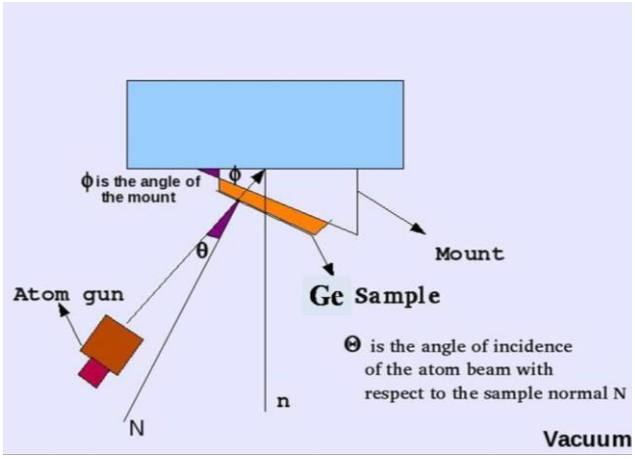

Fig. 1. Schematic of the experimental set-up.

The atom gun is fixed at 45° with respect to the sample normal. For our studies, the angle of incidence of the atom beam has been fixed at 0° with respect to surface normal using a 45° mount on which the samples have been mounted during bombardment. The surface morphologies of the pristine and bombarded samples were investigated by using Atomic Force Microscopy (AFM) Nanoscope IIIa multimode from Digital Instruments. All measurements were conducted in air using Silicon-Nitride tips with a nominal tip radius of < 10nm. The near surface chemical analysis of the pristine and irradiated samples was studied

using X-ray photoelectron measurements in a VG XPS system by utilizing the Mg anode with an overall resolution of 0.9 eV. The range of 1.5 keV Ar atoms inside Ge is ~ 37A^o and the electronic and nuclear energy losses are 3.41 and 26.79 eV/A^o respectively (as estimated by SRIM 2003)[**22**]. Clearly the dominating process is the nuclear energy through which the energy is deposited within the system and the surface morphological changes occur.

Results and discussion

XPS study is carried out for the chemical states identification of elements present in the samples. Elemental survey scan of the pristine sample is shown in the binding energy region of 575-0 eV (shown in **Fig. 2** (i)). All elements present in the sample are indexed in the **Fig.**, which shows that sample is mainly composed of Ge and O elements. The presence of the Cu is because of the substrate holder used in the study. The presence of C is because of the contamination of the sample at surface. For doing the core levels analysis, a Tougaard-type background was subtracted and *XPSPEAK 4.1* program was used. Core level spectra of Ge, in the binding energy region of 36 to 25 eV, have been shown in **Fig. 2** (ii), where spectrum (a), (b), (c) and (d) are corresponding to the pristine and irradiated samples at fluences $5x10^{16}$,$1x10^{17}$ and $3x10^{17}$ atoms/cm^2 respectively. In the spectrum (a), the XPS peak centered at 33.4 eV is assigned to be due to the doublet $3d_{3/2}$ and $3d_{5/2}$ core levels of Ge^{4+} chemically bonded with O. However, we were not able to resolve the splitting of 3d level in $3d_{3/2}$ and $3d_{5/2}$ levels. In the pristine sample, the absence of elemental Ge could be possible, because core level photoelectrons can eject out from only a few nm depth in the sample so in that region the main contribution remains as the GeO_2 only due to an oxide layer and underneath Ge present (if it were there) in samples is not observed. As we have bombarded the samples with the energetic particles, the oxide overlayer got removed and we could see the hump on the lower binding energy side. The broad peaks in (b), (c) and (d) are deconvoluted into three main peaks, where the two new peaks at 29.8 eV and 30.4 eV arise from the doublet of Ge $3d_{5/2}$ and Ge $3d_{3/2}$ core levels. The O (1s) core levels as shown in **Fig. 2** (iii) reveal the presence of GeO_2 at the near-surface. After the deconvolution of broad peak in two components centered at binding energy at 531.0 eV and at 532.0 eV have been found which were attributed to be due to O chemically bonded with Ge and physisorbed O. The binding energies of such assigned Ge and O core levels are consistent with previous results [**23-29**]. When we compared the area under the Ge^{4+} and Ge core level peaks in (a)-(d) spectra (as shown in **Fig. 2** (iv)), a drastic decrease from 51.8 in pristine sample to systematic decrease from 0.34 to 0.27 is observed with the increase in fluences from $5x10^{16}$ to $3x10^{17}$ atoms/cm^2 respectively. Hence, we can conclude from the XPS results, that irradiation with low energy ions leads to the reduction of surface oxide layer into elemental Ge.

The 3d views of the AFM micrographs of the pristine and irradiated samples are shown in **Fig. 3**. **Fig. 3a** shows the morphology of the pristine sample of Ge (100). It can be seen that the surface is not completely flat and shows rms roughness 0.2 nm with few structures on the surface. **Fig. 3**(b, c, d, e, f) shows the morphology at different fluences ($5x10^{15}$, $1x10^{16}$, $5x10^{16}$, $1x10^{17}$ and $3x10^{17}$ atoms/cm^2 respectively. For the initial fluences (upto $1x10^{16}$ atoms/cm^2) there is no significant change in rms roughness of the surface. However, after a fluence of $5x10^{16}$ atoms/cm^2, there is a sharp increase in the roughness value from 4 nm to 10 nm. There is formation of bigger structures due to the self assembly of smaller structures which led to increase in surface roughness.

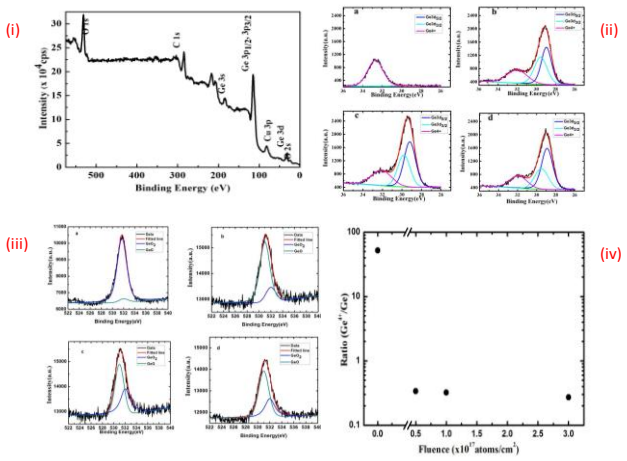

Fig. 2. (i) XPS survey scan of the Ge sample, (ii) XPS spectra of the pristine and irradiated samples :; a) Pristine, b) $5x10^{16}$, c) $1x10^{17}$ and d) $3x10^{17}$atoms/cm^2, (iii) XPS spectra of the pristine and irradiated samples of O-1s :; a) Pristine, b) $5x10^{16}$, c) $1x10^{17}$ and d) $3x10^{17}$atoms/cm^2, (iv) Variation of relative contributions Ge^{4+}/ Ge with respect to atom fluence

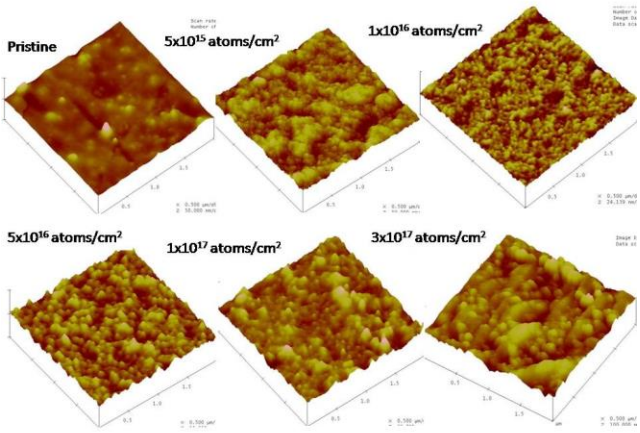

Fig. 3. 3D view of the AFM micrographs of the pristine and irradiated samples

The morphology of the surface is also changed with increasing fluence and formation of nanodots on the surface is clearly seen at highest fluence. Nanostructuring of the surface occur due to the interplay between ion induced sputtering and surface diffusion. The roughness alone gives insufficient information about the change in morphology as it is 2-dimensional (2D) information in *x* and *y* planes. It is a numerical parameter and depends on the scan size. To get the complete information and better understanding of nanostructured surface under the energetic atom bombardment, power spectral density (PSD) was deduced from the AFM micrograph and tries to study the changes observed in the morphology. PSD can provide quantitative

information about the surface roughness in both the vertical and lateral directions and is independent of the scan size. The 2D PSD function is defined as [**30**]-

$$PSD(y) = \frac{1}{area}\left[\iint \frac{d^2r}{2\pi} e^{-iqr}\langle h(r)_t\rangle\right]^2, \quad r = (x,y)$$

where q is the spatial frequency (nm^{-1}) and $h(r)$ is the surface height at a point r.

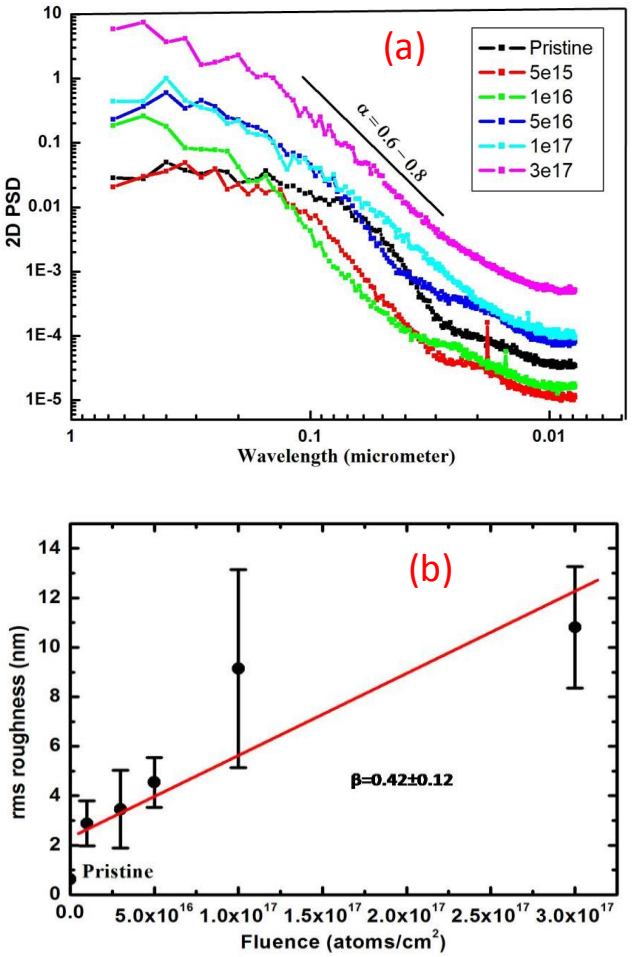

Fig. 4. (a)Log plot of Power spectral density Vs. Spatial wavelength of the pristine and irradiated samples and (b) Log plot of the rms roughness Vs. the atom fluence.

The scan sizes of 2μm × 2μm and 512 × 512 data points were used to scan the samples in AFM. The scaling behavior of the Ge samples was analyzed using PSD curves obtained from AFM images by extracting the values of roughness exponent, α, and growth exponent, β. The exponents, α and β, give spatial and temporal evolution of the structures, respectively. The log plot of 2D PSD function versus spatial frequency is shown in **Fig. 4a**. The horizontal low frequency part shows the uncorrelated white noise that arises due to random arrival of ions onto the surface. There is an increase in the intensity of the plateau with increase of fluences from 5×10^{15} to 3×10^{17} atoms/cm^2, which indicates an increase in roughness. The high frequency linear part shows correlated surface features. The PSD curves do not show any significant peaks corresponding to the nanodot structures which show that the structures lacks the selection of particular wavelength [**31**] and follows power law dependence [**32**]. Hering et al. have shown that slope (n) can have values 1, 2, 3 and 4 which represent different modes of surface diffusion like viscous flow, evaporation-condensation, volume diffusion and surface diffusion respectively [**33**]. The value of n for the different curves of PSD function was calculated to be in the range of 3.2–3.7 for higher fluences and 2.44-2.34 for pristine and lowest fluence. The exponent α was determined using the relation, $\alpha = (n - d)/2$, where n is the slope obtained and d is the dimension of PSD taken from AFM images. The value of α was found to be between 0.6 and 0.9. The value of roughness exponent increases with an increase in fluence. The value of roughness exponent 0.6 can be described by continuum theories, which predict the values of α = 0.38, 2/3 and 1 [**34**]. Moreover, application of ion bombardment results in increment of roughness exponent to 0.9. This high value of α indicates that as the ions are bombarded on the surface, the ion-enhanced surface diffusion term dominates. The surface becomes rough due to the effect of ion induced diffusion for higher fluences leads to coalence of the smaller structures. The growth parameter, β, was determined by plotting rms surface roughness of the pristine and irradiated samples versus ion fluence in log scale (**Fig. 4b**). The slope gives the value of β which was found to be 0.42 ± 0.*12*. This value of β also suggests that the diffusion induced due to ion bombardment dominates. The Edward–Wilkinson (EW) equation [**35**] shows the same scaling properties; in this regime, non-linear effects eventually stabilizes the surface and surface relaxation takes place by diffusion with β = 0.3. The scaling parameter, $z = \alpha/\beta$, was found to be 0.9/0.4 = 2.*25*. The Ge samples follow the scaling behavior as mentioned in the KPZ equation, given by Kardar et al. [**36**], the modified BH equation. The high values of scaling exponent also indicate the anomalous growth of surface under the ion bombardment.

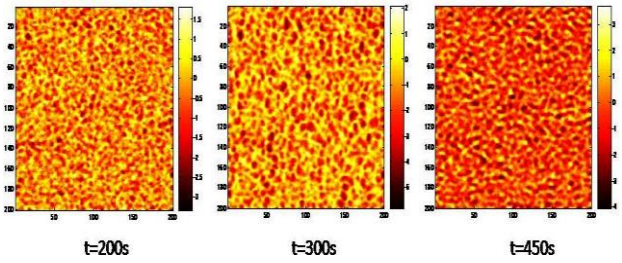

Fig. 5. Simulation results using KS equation

The ion bombarded surface gets roughened due to incoming ions and counter to that the adatoms movements smoothens the surface may be due to annihilation of the surface vacancies. Surface adatoms and surface vacancies contribute equally to static surface topography but in different ways. An isolated adatom introduces the same roughness to the surface as the isolated vacancy. However, the dynamic evolution of the surface morphology under a flux of adatoms is determined by the migration and interaction of the surface defects they create. It has been observed that the kinetics of ion beam roughening is similar

to those of growth roughening [**13**]. We also tried to simulate the results obtained with AFM using the KS equation. **Fig. 5** gives the simulated images at three time scales t=200, 300 and 450 s. The simulation uses a grid size of 200 with δx=δy=1 and δt=0.01. As shown in the images, the surface initially starts deforming at initial time scale with fewer pits and this gradually develops into a regular surface with simultaneous formation of pits and dots. There is an increase in roughness from 0.2 nm to 4 nm for the two fluences.

Conclusion

The surface roughness of the irradiated samples is found to increase with atom fluence due the agglomeration of the smaller surface structures to the bigger structures. This happens due the ion induced surface diffusion process during the bombardment. The size of the nanostructures increases from 60 nm to 100 nm as the fluence is increased. The scaling laws have been investigated and the power law dependence is observed. The surface coarsens as the fluence is increased. The roughness and growth exponents were found to be 0.6 to 0.9 and 0.42 ± 0.13 experimentally. Both the processes, sputtering and ion induced surface diffusion are playing significant roles in the two distinct regimes. For initial fluence, the sputtering dominates and for higher fluences, ion enhanced diffusion leads to mobility causing the structures to broaden with increase in fluence. XPS study shows that there is a transition from Ge^{4+} to elemental Ge as we are observing the pristine to irradiated samples. The result shows analogy with the K-S equation as value of α is found to be lying between the regimes where the mound coarsening is predicted. Simulation also showed the same results as obtained in the AFM micrographs using the KS equation.

Acknowledgements

The author would like to thank Dr. Shikha Varma for her help and discussions for XPS measurements. The financial support from DST under IRPHA project for the SPM facility at IUAC, New Delhi is gratefully acknowledged.

Reference

1. Navez, M.; Sella, C.; Chaperot, D. *C.R. Acad. Sci., Paris* **1962,** 254, 2401
2. Valbusa, U.; Boragno, C.; Buatier de Mongeot, F. J. *J. Phys.: Condens.Matter* **2002,** 14, 8153. **DOI**: 10.1088/0953-8984/14/35/301
3. Facsko, S.; Dekorsy, T.; Koerdt, C.; Trappe, C.; Kurz, H.; Vogt, A.; Hartnagel, H. L. *Science* **1999,** 285, 1551. **DOI***:* 10.1126/science.285.5433.1551
4. Carter; G.; *J. Phys. D:Appl. Phys.* **2001**, 34, R1; **DOI**:10.1088/0022-3727/34/3/201
5. Frost, F.; Schindler, A.; Bigl, F. *Phys. Rev. Lett.* **2000,** 85, 4116. **DOI**:10.1103/Phys. Rev. Lett. 85.4116
6. Gago, R.; Vázquez, L.; Cuerno, R.; Varela, M.; Ballesteros, C.; Albella, J. M.; *Appl. Phys. Lett.* **2001,** 78, 3316. **DOI**:10.1063/1.1372358
7. Frost, F.; Ziberi, B.; Höche, T.; Rauschenbach, B.; *Nucl. Instrum. Methods Phys. Res. B* **2004**, 16, 9 **DOI:**10.1016/j.nimb.2003.11.014
8. Ziberi, B.; Frost, F.; Rauschenbach, B.; Hoche, Th. *Appl. Phys. Lett.* **2005**, 87, 033113 **DOI**:10.1063/1.2000342
9. Sulania, I.; Tripathi, A.; Kabiraj, D.; Varma, S.; Avasthi, D K. Journ. Nanosci. Nanotech. **2008**, 8(8), 4163. **DOI**: http://dx.doi.org/10.1166/jnn.2008.AN13
10. Sulania, Indra; Tripathi, Ambuj; Kabiraj, D.; Lequeux Matthieu; Avasthi Devesh; *Adv. Mat. Lett.* **2010**, 1(2), 118. **DOI**:10.5185/amlett.2010.5128
11. Hazra, S.; Chini, T. K.; Sanyal, M. K. *Phys. Rev. B* **2004**, 70, 121307. **DOI**:10.1103/PhysRevB.70.121307
12. Erlebacher, J.; Aziz, M. J.; Chason, E.; Sinclair, M. B.; Floro, J. A. *Phys. Rev. Lett.* **1999**, 82, 2330. **DOI**:10.1103/PhysRevLett.82.2330
13. Ziberi, B.; Frost, F.; Rauschenbach, B. *Appl. Phys. Lett.* **2006**, 88, 173115. **DOI**: 10.1063/1.2199488
14. Chason, E.; Mayer, T M.; Kellerman, B K.; McIlroy D T.; Howard, A J. *Phys. Rev. Lett.* **1994,** 72, 3040. **DOI**:10.1103/PhysRevLett.72.3040
15. Yang, M.; Wu, R. Q.; Chen, Q.; Deng, W. S.; Feng, Y. P.; Chai, J. W.; Pan, J. S.; Wang, S. J.; *Appl. Phys. Lett.* **2009**, 94, 142903: **DOI**:10.1063/1.3115824
16. Floro, J. A.; Kellerman, B. K.; Chason, E.; Picraux, S. T.; Brice, D. K.; Horn, K. M. *J. Appl. Phys.*, **1995,** 77, 2356. **DOI**: 10.1063/1.358757
17. Chason, E.; Tsao, J. Y.; Horn, K. M.; Picraux, S. T. *J. Vac. Sci. Technol. B* **1989**, 72, 332. **DOI**: 10.1116/1.584744
18. Chason, E.; Tsao, J. Y.; Horn, K. M.; Picraux, S. T.; Aatwater, H A. *J. Vac. Sci. Technol. A*: **1990**, 8, 2507. **DOI**:10.1116/1.576724
19. Zhou, W.; Cuenat, A.; Aziz, M J. Microscopy of Semiconducting Materials 2003: Proceedings of the 13th International Conference on Microscopy of Semiconducting Materials, Cambridge University, 31 March - 3 April **2003**, ed. A. G. Cullis and P. A. Midgley, Institute of Physics and IOP Publishing.
20. Miyawaki, Ako.; Zamri, M.; Hayashi, T.; Hayashi, Y.; Tanemura, M.; Tokunaga, T. Surface and Coatings Technology **2011,** 25, 812. **DOI**:10.1016/j.surfcoat.2011.04.022
21. Kabiraj, D.;.Abhilash, S.R.;.Vanmarcke, L.; Cinausero, N.; Pivin, J.C.;.Avasthi, D.K. *Nucl. Instrum. Methods in Phys. B* **2006**, 244, 100: **DOI**:10.1016/j.nimb.2005.11.018
22. J.F .Zie gler, *SRIM* 17 (2003), http://www.srim.org/
23. Prabhakaran, K.; Ogino, T. *Surf. Sci*. **1995,** 325, 263. **DOI**:10.1016/0039-6028(94)00746-2
24. Perego, M.; Scarel, G.; Fanciulli, M.; Fedushkin, I. L.; Skatova, A. *Appl. Phys. Lett.* **2007,** 90, 162115. **DOI**:10.1063/1.2723684.
25. Delabie, A.; Bellenger, F.; Houssa, M.; Conard, T.S.; Elshocht, V.; Caymax, M.; Heyns, M.; Meuris, M. *Appl. Phys. Lett.* **2007,** 91, 082904. **DOI**:10.1063/1.2773759.
26. Molle, A.; Nurul Kabir Bhuiyan, M.; Tallarida, G.; Fanciulli, M.; *Appl. Phys. Lett.* **2006**, 89, 083504. **DOI**:10.1063/1.2337543.
27. Schmeisser, D.; Schnell, R. D.; Bogen, A.; Himpsel, F. J.; Rieger, D.; Landgren, G.; Morar, J. F. *Surf. Sci.* **1986,** 172, 455 **DOI**:10.1016/0039-6028(86)90767-3
28. Craciun, V.; Boyd, I. W.; Hutton, B.; Williams, D.; *Appl. Phys. Lett.* **1999,** 75, 1261. **DOI**:10.1063/1.124661.
29. Hidalgo, Pedro; Liberti, Emanuela; Rodrı´guez-Lazcano, Yamilet; Me´ndez, Bianchi; Piqueras, Javier**;** *J. Phys. Chem. C* **2009** *113*, 17200–17205. **DOI:** 10.1021/jp905587c
30. Petri, R.; Brault, P.; Vatel, O.; Henry, D.; Andre, E.; Dumas P.; Salvan, F.; *J. Appl. Phys*. **1994,** *75*, 7498. **DOI**:10.1063/1.356622
31. Agarwal, D C.; Chauhan, R S.; Avasthi, D K.; Khan, S A.; Kabiraj, D.; Sulania, I. J Appl. Phys. **2008,** *104*, 024304. **DOI**: 10.1063/1.2953177
32. Eklund, E A.; Snyder, E J.; Williams, R S; *Surf. Sci.* **1993,** *285*,157. **DOI**:10.1016/0039-6028(93)90427-L
33. Herring, C. *J. Appl. Phys*, **1950,** 21, 301.; doi: 10.1063/1.1699658
34. Barabasi, A L; Stanley H E. *Fractal Concepts in Surface Growth*. Cambridge University Press, **1995** - Science- 366 pages
35. Choudhary, Y.S.; Khan, S.A.; Srivastava, R.; Satsangi, V.R.; Prakash, S.; Avasthi, D.K.; Dass, S. *Nucl. Instrum. Methods B* **2004,** *225*, 291. **DOI**:10.1016/j.nimb.2005.11.034

36. Kardar, M.; Parisi, G.; Zhang, Y. C. *Phys. Rev. Lett.***1986,** *56*,889.
DOI:10.1103/PhysRevLett.56.889

